

# Evaluating the Performance of High Level-of-Detail Tree Models in Microclimate Simulation

H. Xu<sup>1</sup>, C.C. Wang<sup>1,\*</sup>, X. Shen<sup>2</sup> and S. Zlatanova<sup>1</sup>

<sup>1</sup> School of Built Environment, University of New South Wales, Sydney, NSW 2052, Australia – (han.xu8, cynthia.wang, s.zlatanova)@unsw.edu.au

<sup>2</sup> School of Civil and Environmental Engineering, University of New South Wales, Sydney, NSW 2052, Australia – x.shen@unsw.edu.au

## Commission IV, WG IV/9

**KEY WORDS:** Microclimate Simulation, Urban Vegetation, Model Evaluation, Tree Reconstruction, Level of Detail.

### ABSTRACT:

Present urbanization influences urban morphology by the increasing number of dense buildings and infrastructure, which effects climate change. Microclimate simulations including urban vegetation help in mitigating climate change. Most of existing microclimate simulations simplify trees and thereby may introduce some erroneous estimates. Tree models of high levels of detail (LOD) can provide a more accurate measure. Technology advances make it possible to reconstruct detailed tree models, which can be further used in microclimate simulations. However, the few studies presenting detailed tree models focus predominantly on the reconstruction process and omit the microclimate simulations. The objective of this study is to investigate high LOD tree models in microclimate simulation to estimate the potential gain in accuracy. This study focuses on voxel-based tree models and microclimate simulations using computer fluid dynamics software. A series of microclimate simulations are completed in two scenarios, which are single tree and a set of trees with buildings. Based on the simulation results, the advantages of detailed voxel tree models are demonstrated. Final discussion elaborates on the needed and preferred levels of detail for tree models.

## 1. INTRODUCTION

With increasing urbanization, densely built-up fabrics and infrastructure, artificial surfaces with high surface varieties characterize the urban morphology (Chorianopoulos et al., 2010; Stewart, Oke, 2012). Such changes of urban morphology contribute to the climate change in many ways, for example, increasing energy and water use, provide unsatisfactory indoor and outdoor thermal comfort, which lead to decreased health conditions and wellbeing (Barati, Shen, 2016; Wang et al., 2019). Increasing green infrastructures is one of the measures taken for counteracting the climate change due to their ability of regulating the microclimate (De Carvalho, Szlafsztein, 2019). Urban vegetation reduces the sun radiation absorbed by buildings and grounds, cools the air and ground temperature through the evaporation and considerably modifies the wind field in urban areas.

Microclimate simulations are crucial to analysing and predicting urban morphology and provide estimates for the level of climate change. They offer urban planners a better understanding of local climate conditions and predict the possible change brought by the planned measures (Yang et al., 2020). The accuracy of the simulations affects subsequent decision-making in urban planning. Generally, microclimate simulations involve urban vegetation for the better prediction and the optimization of planting patterns. In most of existing microclimate simulations, trees are usually represented by simple shapes (e.g., circular shapes) with several approximate parameters (e.g., LAD, height, crown radius, view factors, etc.) (Xu et al., 2021a). This kind of simplification seeks for a balance between resolution and performance. However, more details, such as trees' geometric features, physiological characteristics and the relation to the surroundings are needed for a comprehensive analysis of

microclimate (Xu et al., 2021a). The used approximations in simplified tree models cause inaccuracy of the simulation results.

Recent years have seen the sophistications of information and communication technology, ubiquitous technologies, and the Internet of Thing (Chourabi et al., 2012; Meng et al., 2021; Pan et al., 2021; Shirowzhan et al., 2017; Wang et al., 2021a; Xu et al., 2021b). In that case, some advanced concepts such as Digital Twin and Smart City emerge. They offer means to create and maintain realistic digital city models. Light Detection and Ranging (LiDAR) or photogrammetry offers point clouds with reliable spatial information for a wide range of built environment applications already (Sepasgozar et al., 2016; Wang et al., 2020a; Wang et al., 2021b; Xu et al., 2021c). Supported by advanced technology, now it is possible to reconstruct 3D realistic tree models from point clouds (Barton et al., 2020; Boufidou et al., 2011; Eusuf et al., 2020; Homainejad et al., 2022; Wang et al., 2020b). The reconstructed tree models have accurate height and width of canopy compared to those represented by simple shapes. Furthermore, the reconstructed tree models have the realistic canopy morphology which preserves more details of the crown (Chakraborty et al., 2019; Janoutová et al., 2019). Adopting detailed tree models into microclimate simulations will increase the accuracy and will help to specific and definitive decision-makings on urban management or planning.

However, including realistic tree models in microclimate simulations costs significantly more time and computational power. Besides, the computational effort and requirement of raw point clouds differ in terms of the reconstruction approach and the LOD of reconstructed tree models. Extensive literature review shows that currently only few studies have applied detailed tree models in microclimate simulations. Currently, it is unknown by what degree the simulation accuracy has been improved by increasing the LOD of tree models. If the tree

---

\* Corresponding author

models are too detailed, it may increase too much the computational effort for a neglectable improvement. On the other hand, if tree models are overly simplified, the simulation results may deviate far away from the reality. Therefore, a balance of LOD of tree models and the desired accuracy of simulation results needs to be found.

The objective of this study is to adopt detailed tree models for microclimate simulations. Specifically, we evaluate the impact of high LOD tree models, with a relatively complex canopy morphology, on the accuracy of microclimate simulations. The paper starts by defining circumstances in which detailed tree models are needed. It delineates the trees' impact is significant and sensitive to the LOD of tree models. Then the paper compares the simulations using detailed tree models and simplified tree models respectively. Finally, this study also discusses how to simplify trees.

## 2. EXPERIMENTAL SETUP AND WORKFLOW

This study aims to assess the potential need of adopting LOD 3 trees in microclimate simulations. Hence, the necessity of LOD 3 trees is evaluated through the comparison between LOD 2 trees, which are commonly used in existing simulations. Two assumptions are introduced: 1) The LOD 3 trees are reconstructed from point clouds of real trees, which are more accurate representation of real trees than simplified and hypothetic tree models. 2) The LOD3 trees results in equal or more accurate simulation results. Therefore, this study focuses on examining how much difference LOD3 model will give in comparison with the LOD2 model. While this paper does not provide validation of the LOD3 model by actual microclimate data, it draws conclusions on whether higher LOD level of tree models can make significant difference in microclimate simulation, especially, for a relatively small precinct area.

Two environmental scenarios are considered: Scenario A and Scenario B. Scenario A represents an individual tree without other urban objects. It is designed to explore the effect of the LOD of individual tree. By contrast, Scenario B is designed to evaluate a more realistic situation, i.e., a set of trees with buildings.

Figure 1 illustrates the two scenarios. Scenario A (Figure 1 a), occupies a 100m×100m×30m space, while Scenario B (Figure 1 b) covers a 170m×80m×40m space. The ground surface is set to asphalt road and the buildings are assumed to be built by cast dense concrete. The surface and building materials used are given with their default values in the simulation software. Series of simulations for both scenarios are performed.

### 2.1 Experimental Setup

Nine different trees are created using voxels of 1×1×1 m. This size was imposed by the simulation software. The trees have different dimension and representation, while the other parameters, needed for the simulation, remain constant, as listed in Table 1. The tree LOD are based on the refined definition of vegetation LOD as given in (Ortega-Córdoba, 2018). LOD 2 trees are pre-made models that have a regular shape and are not acquired from the reality. They can reflect the genus or species form and are scaled in height and width. By contrast, LOD 3 trees are defined to be acquired based on real-world objects, point cloud based and have an irregular shape or form.

Five trees are manually created, as shown in Figure 2. They all model a Eucalyptus, one of the common street tree species in

Australia, with different canopy geometries. For convenience, these canopy geometry types are labelled as Types 1 – 5. Type 1 tree is assumed as a realistic voxel-based LOD 3 model acquired from point clouds. It has irregular canopy morphology with gaps in the crown. While Types 2 – 5 trees are the LOD 2 models represented by regular shapes (cylinder, sphere, cone and inverted cone) and describe in-crown structure little.

Settings	Value
CO2 fixation	C3
Leaf type	Deciduous leaf
Leaf area density in each 3D grid	1m <sup>2</sup> /m <sup>3</sup>
Foliage shortwave albedo	0.18
Foliage shortwave transmittance	0.30
Leaf weight	100g/m <sup>2</sup>
Isoprene Capacity	12

Table 1. Generic and constant tree settings.

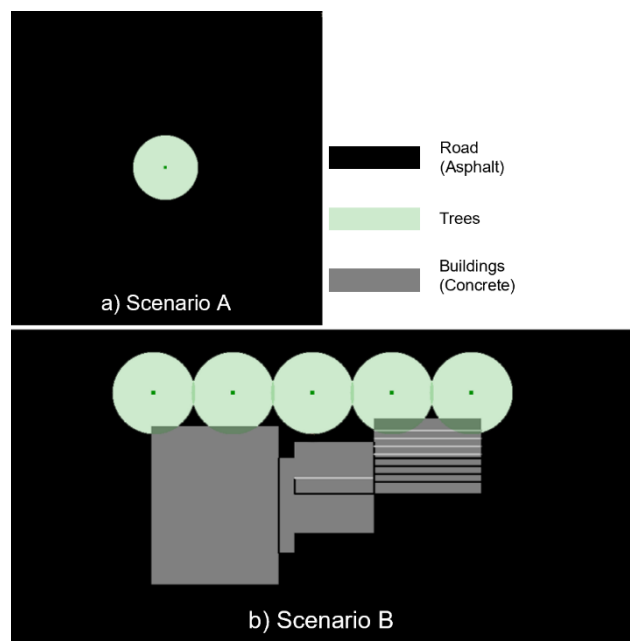


Figure 1. Layouts of Scenario a) A and b) B.

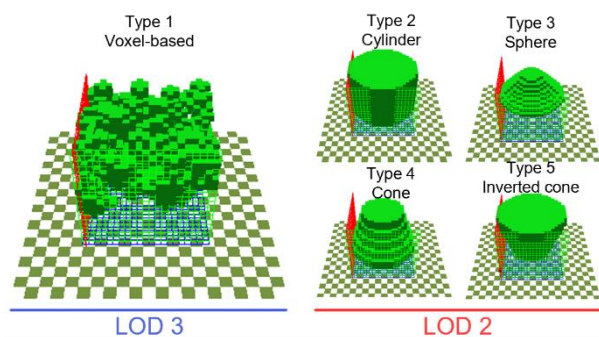


Figure 2. Five trees used in the microclimate simulations.

Table 2 lists the 12 cases and tree parameters used. In some cases, LOD 2 and LOD 3 trees have same dimension. This might be no always the case, because both LOD 2 and LOD 3 are approximations. Consequently, errors in trees' dimensions are unavoidable. However, we assume that trees of different LOD can have the same size and height. This makes the conclusions

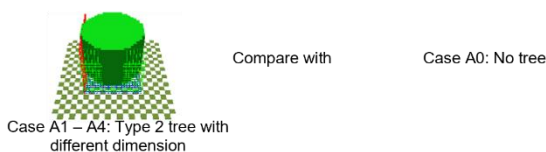
conservative because greater differences between trees of different LODs cause larger error in simulations. Grouping of cases and their corresponding objectives are listed in Table 3. The 10 cases are organised into 3 groups for comparison in Scenario A. The case comparisons in each Group are explained below and visually illustrated in Figure 3:

(1) In Group 1, Cases A1 – A4 are compared to Case A0 to show the difference in microclimate before and after planting a tree. Case A0 has no trees while Cases A1 – A4 have a single cylinder-represented tree.

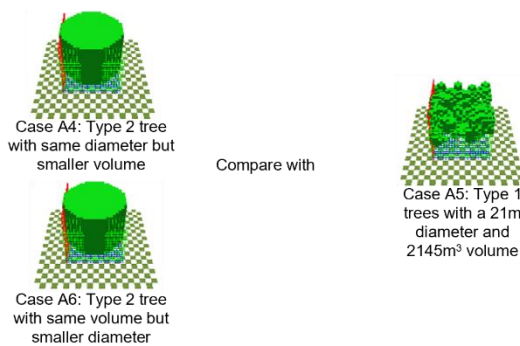
(2) Cases A4 and A6 are compared in terms of the disparity with Case A5 in Group 2. Cases A4 and A6 both have simplified cylinder-represented tree. What makes a difference is that the tree in Case A4 has the same diameter as Case A5, while the tree in Case A6 has the same volume as Case A5.

(3) Cases A4, A5 and A7 – A9 are included in Group 3. They all use the trees of the same dimension. Case A5 adopts the LOD 3 tree, while Cases A4 and A7 – A9 adopt the LOD 2 trees represented by different shapes (see Type 2 – Type 5 listed in Figure 2). Cases A4 and A7 – A9 are compared to Case A5 to assess the performance of LOD 3 tree. They are also compared to themselves to assess the performance of different simplification shapes.

**Group 1**



**Group 2**



**Group 3**

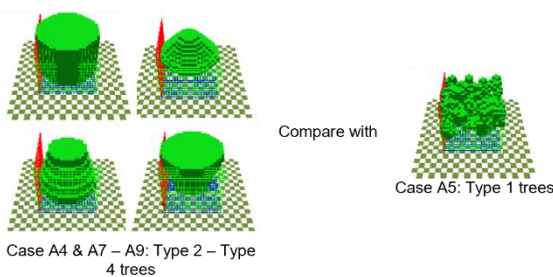


**Figure 3.** Visual illustration of tree models in each group.

There are two cases, Cases B1 and B2 that are used for Scenario B. Instead of adopting 4 LOD 2 trees in Scenario B, Case B1 uses

cylinder-represented trees as a proxy. By contrast, Case B2 adopts LOD 3 trees of the same dimension.

**2.2 Assessment Criteria**

Microclimate is complex to assess and many factors should be considered such as air temperature, mean radiation temperature, wind speed, relative humidity, etc. In this study, Physiological equivalent temperature (PET) is used to assess the microclimate synthetically. PET is a single index that quantifying the thermal effect of a given microclimate (Deb, Ramachandraiah, 2011). It expresses the environment in terms of indoor temperature without wind and solar radiation, which gives a more intuitive and easy impression of microclimate for people to imagine with their common experience. The PET is calculated with respect to a male who stands 1.75 m tall and the PET at 1.5m above the ground, where the PET change can be felt, is recorded as a comparison indicator.

Case	Trees parameters				
	Canopy geometry type	LOD	Canopy top height (m)	Canopy base height (m)	Canopy diameter (m)
A0	No trees	/	/	/	/
A5, B2	1	3	20	5	21
A1	2	2	5	1	5
A2	2	2	10	3	11
A3	2	2	15	4	15
A6	2	2	20	5	13
A4, B1	2	2	20	5	21
A7	3	2	20	5	21
A8	4	2	20	5	21
A9	5	2	20	5	21

**Table 2.** Trees parameters in each case.

Scenario	Group	Cases	Objective
A	1	A0 – A4	Identify the general range of individual tree’s impact.
	2	A4 – A6	Retain diameter or volume in LOD 2 trees.
	3	A4, A5 & A7 – A9	Compare LOD 2 trees represented by different regular shapes. Compare LOD 2 and LOD 3 individual tree.
B	/	B1 & B2	Identify the general range of clustered trees’ impact. Compare a set of LOD 2 and LOD 3 trees.

**Table 3.** Case comparison in each Group and corresponding objectives.

The term thermal sensitivity is used to assess the PET change. It is defined as the occupant’s sensitivity to changes in indoor temperature (Rupp et al., 2022). It quantifies the change in the thermal sensation of occupants in response to per unit of room temperature change ( $^{\circ}\text{C}^{-1}$ ). Thermal sensitivity is related to many factors (e.g., building occupancy type and location, etc.) and therefore hard to determine. As a compromise, it is taken as a constant value of  $0.5^{\circ}\text{C}^{-1}$ , called Griffiths Constant. Griffiths Constant is based on both the SCATS and ASHRAE RP-884 databases (Humphreys et al., 2013) and has been widely used in thermal comfort studies. It means  $2^{\circ}\text{C}$  change in indoor temperature changes 1 unit in the thermal sensation scale. The common thermal sensation scales are listed in Table 4. Based on

the Griffiths Constant, an assessment criterion is customized to assess the PET change as listed in Table 5.

Thermal sensation scale	ASHRAE scale	Bedford scale
3	Hot	Much too warm
2	Warm	Too warm
1	Slightly warm	Comfortably warm
0	Neutral	Comfortable
-1	Slightly cool	Comfortably cool
-2	Cool	Too cool
-3	Cold	Much too cold

**Table 4.** Common thermal sensation scales used in comfort research.

PET change (°C)	Assessment
$-1 < \Delta\text{PET} < 1$	Slight
$-2 \leq \Delta\text{PET} < -1$ or $1 < \Delta\text{PET} < 2$	Intermediate
$\Delta\text{PET} \geq 2$ or $\Delta\text{PET} \leq -2$	Significant

**Table 5.** Assessment criterion for PET change.

### 2.3 Simulation Software

All microclimate simulations are conducted on a computer with 32 GB of RAM and an Intel (R) Core (TM) i9 – 10850K CPU. A commercial software ENVI-met 4.4.6 is used to complete the simulations. The software uses Computational Fluid Dynamic (CFD) model to simulate urban thermal environment characteristics (Bruse, Fler, 1998). It simulates the surface-vegetation-atmosphere interactions and has relative well-conceived vegetation sub-models. It is considered as a helpful tool for urban climate analysis which is receiving increasing popularity in urban mid-scale microclimate simulation (Tsoka et al., 2018).

The simulations are done for a summer day in Sydney, 14<sup>th</sup> Jan. The meteorological data refers to climate data developed for the Australia Greenhouse Office for use in complying with Building Code of Australia (U.S. Department of Energy, 2022). The simulation period is set from 8:00 to 16:00, where the max sun radiation and wind speed are included. The time zone is set in the UTC/GMT+10 and the corresponding sunrise and sunset times automatically generated are 5:00 and 17:00 respectively. The sun radiation, wind speed and wind direction at 8:00, 12:00 and 16:00 are listed in Table 6.

Time	8:00	12:00	16:00
Direct sun radiation (W/m <sup>2</sup> )	967.92	735.09	565.55
Diffuse sun radiation (W/m <sup>2</sup> )	124.00	220.50	119.00
Wind speed (m/s)	0	3.9	4.7
Wind direction (°)	0	45	45

**Table 6.** Meteorological data at specific times.

### 3. SIMULATION RESULTS FROM SCENARIO A

In this section, Cases A0 – A9 are compared as explained in Section 2.1 to estimate the effect of a single tree of different parameters.

#### 3.1 Impact of trees

Table 7 illustrates the PET of Cases A1 – A4 subtracted from Case A0. The comparison between Cases A4 and A0 are given in the second row as an example. Significant PET changes can be observed in the zone near the trees, marked by dark blue and light

purple. For most of the zone, the PET drops significantly by more than 2°C, with a small percentage under the canopy rising by more than 2°C. In the rest of the space, the change in PET is only slight or intermediate within ±2°C. This zone is, hence, identified as the impact zone. The minimum PET change is seen at 8:00, when the tree reduces the PET by 21.35°C.

The range of the impact zone is given by two indicators, *a* and *b*, to describe its length and width respectively. The indicator *a* is the distance from the farthest end of the impact zone to the center of the tree along the extension direction of the impact zone. The indicator *b* is the widest distance perpendicular to this direction.

Time	Result of Case A4	Case	A1	A2	A3	A4
8:00		<i>a</i> (m)	9	19	29	39
		<i>b</i> (m)	5	11	15	22
12:00		<i>a</i> (m)	4	8	11	16
		<i>b</i> (m)	5	10	14	21
16:00		<i>a</i> (m)	5	14	23	32
		<i>b</i> (m)	5	10	16	21
Legend						

**Table 7.** PET of Cases A1 – A4 subtracted from Case A0.

The impact zone depends on the tree dimension. Table 7 shows a clear relationship between *a* and the tree height. At 8:00 and 16:00, *a* usually equals twice the tree height while at 12:00, *a* is slightly larger than the tree diameter. During the whole simulation period, *b* always coincides with the diameter of the tree approximately. Besides, the impact zone is dynamic with the change of environment. Case A4 illustrates that the impact zone takes up relatively large chunks of space at 8:00 and 16:00. By contrast, it just occupies a circle slightly larger than the canopy at 12:00. It can be seen in all Cases A1 – A4 the impact zone shifts from west to east, changing its range.

Since PET is a combination of air temperature and wind speed, the generation of the impact zone can be explained from these

two parts. The impact zone usually reflects the projection of the tree in the sunlight, where the air temperature is considerably reduced because the canopy blocks the sun radiation. This makes it change with the sun height and sun altitude angle. On the other hand, the impact zone may be slightly modified due to the change of wind speed. However, as shown in Table 7, their generation is dominated by sunlight incidence. Particularly at 16:00 when the wind blows from the northeast and the sun is in the west, the impact zone lies to the east of the tree.

In conclusion, the impact zone can be visually perceived as the shadow of the tree. It extends to twice the tree height on both the east and the west sides in the morning and afternoon. While at noon, it is slighter larger than the canopy at noon.

### 3.2 Comparison in Group 2

Figure 4 illustrates the results from cases A4 and A6 to Case A5. Due to the space limit, only the result at 8:00 is given to show the maximum difference in simulation results. Compared to Case A5, the geometry of the tree in Case A4 is a cylinder with the same diameter but larger volume. Cases A6 considers a tree which retains the volume of the tree but having a smaller diameter. This simplification reveals a significant PET change over  $\pm 2^\circ\text{C}$ , which can be seen in most of the impact zone of both Cases A4 and A6. By contrast, out of the impact zone, replacing LOD 2 trees with LOD 3 trees only causes a PET difference within  $\pm 2^\circ\text{C}$ . The PET change, which does not reach a significant level, is seen in each group and will not be repeated in the following discussion.

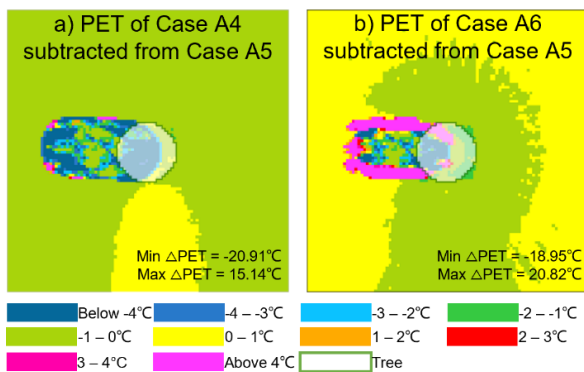


Figure 4. PET of Cases a) A4 and b) A6 subtracted from Case A5.

Time	8:00		12:00		16:00	
Case	<i>a</i> (m)	<i>b</i> (m)	<i>a</i> (m)	<i>b</i> (m)	<i>a</i> (m)	<i>b</i> (m)
A5	38	23	15	21	33	21
A4	39	22	16	21	32	21
A6	34	15	11	13	29	13

Table 8. Rang of the impact zone of Cases A4 – A6.

Although both cases introduce noticeable PET difference, Case A4 performs better than Case A6. Table 8 lists *a* and *b* describing the range of the impact zones in Cases A4 – A6. It is seen that the impact zones in Cases A4 and A5 have similar range, while the one in Case A6 is narrower because of the smaller tree diameter. That explains the significant increase in PET on the edge of the impact zone in Figure 4 b. Therefore, it can be concluded that errors are unavoidable if using LOD 2 trees. But keeping the diameter and height of the tree accurate enables the simulation of a more accurate impact zone.

### 3.3 Comparison in Group 3

Figure 5 demonstrates the comparison of Cases A4, A7 – A9 to Case A5 at 8:00, when the PET difference is the most noticeable. A considerable PET difference can be seen in all cases. Most of the impact zones have a PET difference above  $4^\circ\text{C}$  or below  $-4^\circ\text{C}$ , which is marked by light purple and dark blue respectively. The minimum PET difference drops to  $-20.91^\circ\text{C}$  and the maximum PET difference reaches up to  $20.77^\circ\text{C}$ . This is due to the different canopy geometry of LOD 2 (i.e., Types 2 – 5 trees) and LOD 3 trees (i.e., Type 1 tree), resulting in the inconsistency of the impact zone range. Consequently, there are locally significant PET differences in the impact zone.

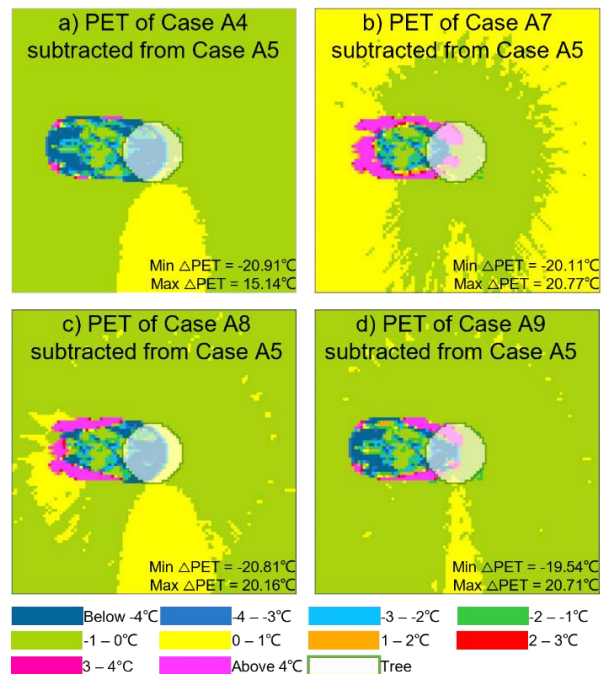


Figure 5. PET of a) Case A4, b) A7, c) A8 and d) A9 subtracted from Case A5 at 8:00.

Table 9 lists the PET of Cases A4 and A7 – A9 subtracted from Case A5 at 8:00, 12:00 and 16:00. The PET differences are significant and similar among cases. As a result, it is hard to determine which type of representation of the LOD 2 tree is superior. In Table 9, there is a trend that the PET difference reaches the minimum at noon from the maximum in the morning. However, it increases again in the evening. This means the PET difference is influenced by both the sun radiation and the range of the impact zone. The reduction in PET difference is because of the decrease in sun radiation.

Time	8:00		12:00		16:00	
Case	Min Δ PET (°C)	Max Δ PET (°C)	Min Δ PET (°C)	Max Δ PET (°C)	Min Δ PET (°C)	Max Δ PET (°C)
A4	-20.91	15.14	-4.49	3.42	-7.41	5.45
A7	-20.11	20.77	-3.89	3.62	-7.24	6.55
A8	-19.54	20.71	-3.56	3.68	-7.41	6.64
A9	-20.81	20.16	-3.82	3.62	-7.15	6.43

Table 9. Minimum and maximum PET difference of Case A4 and A7 – A9 compared to Case A5 at 8:00, 12:00 and 16:00.

The sun radiation, as listed in Table 6, keeps decreasing during the whole simulation time. Therefore, the PET difference is

smaller at 12:00 and 16:00 than at 8:00. On the other hand, the increase in PET difference from 12:00 and 16:00 can be explained by the increase in the range of the impact zone. As shown in Table 8, the impact zone is larger at 16:00 than at 12:00. As a result, the range of the impact zone differs greater from case to case, which amplifies the PET difference.

To summarize, the adoption of the LOD 2 tree introduces errors. These errors cannot be reduced by changing the parameters of the tree. By contrast, LOD 3 tree is able to give a more accurate simulation result. Its irregular canopy morphology with gaps allows to simulate a more exact impact zone with inhomogeneous distribution of PET.

#### 4. SIMULATION RESULTS FROM SCENARIO B

In this section, Cases B1 and B2 are compared. According to the basic findings in Section 3, it is important to ensure that the diameter and height of LOD 2 trees are accurate. And 4 types of LOD 2 trees, i.e., Types 2 – 5 trees, introduce similarly errors. Therefore, in this section, Case B1 uses Type 2 tree, i.e., cylinder-represented, to be the proxy of the simulations using LOD 2 trees. Case B2 uses Type 1 tree, i.e., LOD 3, with the tree parameters as given in Table 2. The five trees in each case have the same properties.

Figure 6 demonstrates the simulation result of Case B2. The impact zone generated in Scenario B can be seen as the aggregation of multiple trees acting individually. Therefore, the impact zone extends to twice the tree height from the center of the tree farthest from the sun. Its range still depends on the sun height, sun altitude angle and wind direction. As a result, the impact zone is large at 8:00 and 16:00, but narrow at 12:00, shifting from west to east from morning to evening. Compared to the Scenario A, the PET differences are more noticeable at two ends and the edge of the impact zone in Scenario B. This is because the trees planted together fill the gaps in their neighbours' canopies.

Figure 7 illustrates the PET of Case B2 subtracted from Case B1. As we assume that it leads to a more accurate simulation with LOD 3 trees, the PET difference between Cases B2 and B1 shows the advantages of LOD 3 trees in potential gains in accuracy. There are significant PET differences above 4°C or under -4°C at a large percent of the impact zone, which is marked by blue and purple. The minimum and maximum PET differences are -24.42°C and 11.66°C respectively, which occurs at 8:00 when the sun radiation is intense. Although the PET difference is lower at 12:00 and 16:00, but they are still over 2°C or below -2°C, which are at the significant level that causes a gap in thermal comfort. It can be concluded that LOD 3 trees are capable of delineating the impact zones and the simulating irregular distributed PET within impact zones, thereby improving the accuracy. In comparison, the PET difference out of the impact zone is intermediate or slight, between -2 – 1°C. This indicates that even when trees are planted in a set, replacing LOD 2 trees with LOD 3 trees still causes limited difference out of the impact zone.

Replacing LOD 2 trees with LOD 3 trees increases the complexity of the entire simulation. However, the difference between simulation times of the two cases is small, as listed in Table 10. This is because every voxel in the space is involved in the calculation during simulation in ENVI-met, regardless of how complex trees are. Therefore, applying LOD 3 trees does not cost too much extra computational effort, at least in ENVI-met. This conclusion may be extended to the CFD models represented by

ENVI-met. In addition, it is reasonable to infer that this conclusion applies to simulations on larger areas. The simulations for Scenario B cover a relatively small area. They focus on the trees' impact on individual buildings or a particular precinct. In this case, small voxel size is commonly used, which leads to sufficient voxel numbers filling the space. By contrast, the microclimate simulations on large areas focus on getting a general picture of the entire areas. Hence, larger voxel sizes are usually adopted to control the number of voxels, which results in trees being certainly simplified. Eventually, the number of voxels in the simulations on larger areas may be similar to the simulations for Scenario B.

Case	Initialization time	Main program run time	Total simulation time
Case B5	5h 49min 43s	81h 55min 44s	87h 45min 27s
Case B6	6h 3min 39s	81h 17min 7s	87h 20min 46s

Table 10. Simulation time of Case B5 and Case B6.

#### 5. CONCLUSIONS AND LIMITATIONS

This study presents a series of microclimate simulations to evaluate the performance of various trees. Two scenarios are considered: one with a single tree and the other several trees next to a building. The results of the simulations allow to conclude on the needed tree details. Trees usually have a greater impact on the zones close to them. Therefore, these zones are referred as to the impact zones. On sunny summer days with intense solar radiation and high sun altitude angle, trees' impact zones can be clearly identified as being the tree shadows. Under such meteorological conditions, the impact zones reach as far as twice the trees' height from the center of trees at morning and afternoon, while is confined to the space a bit larger than canopy coverages at noon.

With LOD 2 and LOD 3 trees, the simulation results have negligible differences out of the impact zone. When assessing the microclimate global rather than for a local space, adopting LOD 2 trees can provide a valuable reference. However, whether it is reliable needs the validation with real data. When adopting LOD 2 trees, it is important to ensure the diameter and height of trees are consistent with the reality. This guarantees the accurate range of the impact zones. Although LOD 2 trees can be represented by different shapes, they still cannot describe the irregular canopy geometry and complex in-crown structure. Consequently, the error resulted is usually unavoidable.

When the microclimate in the impact zones needs to be accurately simulated, LOD 2 and LOD 3 trees lead to significant different results. Such circumstances may include predicting the energy use of buildings near trees and finding out the thermal comfort of pedestrians in the tree shade or the building occupants (Wang, Zamri, 2013). In these circumstances, more detailed tree models are required. Compared to LOD 2 trees, LOD 3 trees have accurate canopy morphology with detailed in-crown structure. Their detailed mode allows to simulate the inhomogeneous distribution of PET in the impact zones. Besides, little additional time is required when replacing LOD 2 trees with LOD 3 tree s in CFD models. This is because CFD models calculate every voxel of trees during simulation, even they are represented by regular shapes. On balance, adopting LOD 3 trees improves the simulation accuracy significantly and cost little extra time. Hence, LOD 3 trees are recommendable as long as it takes acceptable time to reconstruct them.

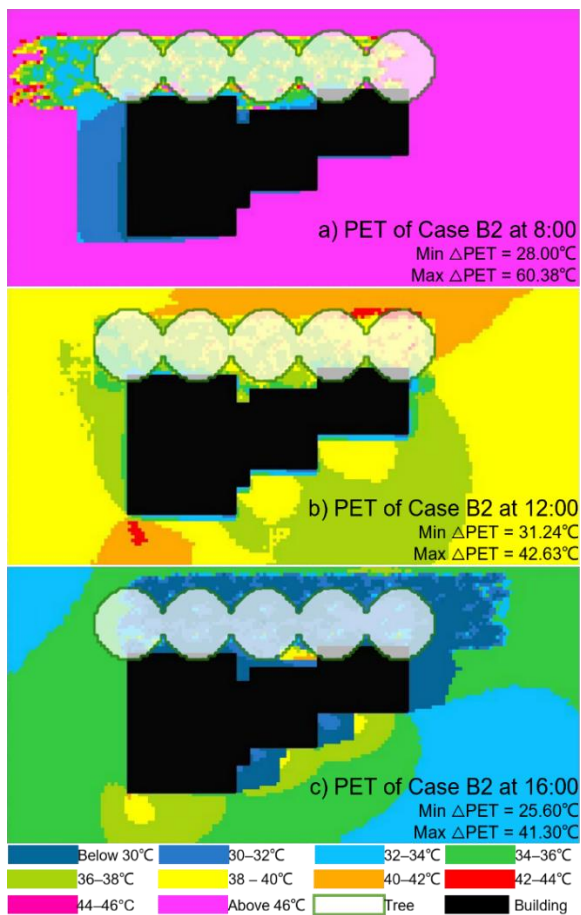


**Figure 6.** PET of Case B2 at a) 8:00, b) 12:00 and c) 16:00.

There are several points for further investigations. First, all microclimate simulations are done in a specific software, i.e., ENVI-met. The smallest voxel size of trees allowed in the software is 1m<sup>3</sup>. The LOD 3 trees with smaller voxel size may have more difference with LOD 2 trees and lead greater gains in accuracy. However, even with the current voxel size, the simulations of a 170m×80m×40m urban environment are already time consuming, requiring more than 87 hours. Using more powerful computers may reduce the simulation time. However, the simulations with smaller voxel size will require excessive computational effort and thus will become less practical.

This study models the daytime during summer, which makes the conclusions time- and place-specific. Future research could be on extending the climatic conditions to cloudy days or winter days and simulating various regions to get more general conclusions.

In addition, this study only considers the visual change of trees. It does not take trees' physiological characteristics (e.g., leaf area density, foliage shortwave albedo and foliage shortwave transmittance, etc.) into account. For example, if trees' LAD is not 1.0m<sup>2</sup>/m<sup>3</sup>, the conclusion may be changed. Besides, LOD 3 trees are supposed to have more accurate physiological characteristics than LOD 2 trees do.

In future work, a sensitivity study of microclimate to trees' physiological characteristics will be conducted to enhance the comments on reconstructed trees. Furthermore, LOD 3 trees will be reconstructed from LiDAR point clouds. The microclimate

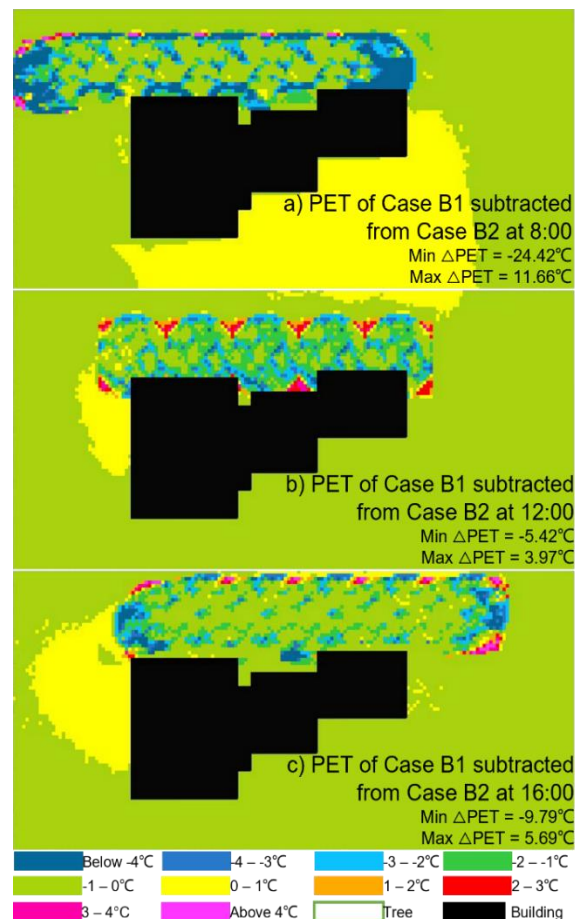


**Figure 7.** PET of Case B2 subtracted from Case B1 at a) 8:00, b) 12:00 and c) 16:00.

data will also be collected by on-site installed sensors. The microclimate simulation results using reconstructed LOD3 models based on laser scanning will be compared with real data for validation.

## REFERENCES

- Barati, K., Shen, X., 2016. Operational level emissions modelling of on-road construction equipment through field data analysis. *Automation in Construction*, 72, 338-346.
- Barton, J., Gorte, B., Eusuf, M. S. R. S., Zlatanova, S., 2020. A voxel-based method to estimate near-surface and elevated fuel from dense LiDAR point cloud for hazard reduction burning. *ISPRS Annals of Photogrammetry, Remote Sensing and Spatial Information Sciences*, VI-3/W1-2020, 3-10.
- Boufidou, E., Commandeur, T., Nedkov, S., Zlatanova, S., 2011. Measure the climate, model the city. *ISPRS - International Archives of the Photogrammetry, Remote Sensing and Spatial Information Sciences*, XXXVIII-4/C21.
- Bruse, M., Fler, H., 1998. Simulating surface-plant-air interactions inside urban environments with a three dimensional numerical model. *Environmental Modelling and Software*, 13(3-4), 373-384.
- Chakraborty, M., Khot, L. R., Sankaran, S., Jacoby, P. W., 2019. Evaluation of mobile 3D light detection and ranging based canopy mapping system for tree fruit crops. *Computers and Electronics in Agriculture*, 158, 284-293.

- Chorianopoulos, I., Pagonis, T., Koukoulas, S., Drymoniti, S., 2010. Planning, competitiveness and sprawl in the Mediterranean city: The case of Athens. *Cities*, 27(4), 249-259.
- Chourabi, H., Nam, T., Walker, S., Gil-Garcia, J. R., Mellouli, S., Nahon, K., Pardo, T., Scholl, H., 2012. Understanding smart cities: An integrative framework. *45th Hawaii International Conference on System Sciences*, 2289-2297.
- De Carvalho, R. M., Szlafsztein, C. F., 2019. Urban vegetation loss and ecosystem services: The influence on climate regulation and noise and air pollution. *Environmental Pollution*, 245, 844-852.
- Deb, C., Ramachandraiah, A., 2011. Review of studies on outdoor thermal comfort using physiological equivalent temperature (PET). *Journal of the Institution of Engineers (India): Architectural Engineering Division*, 92(APRIL), 38-41.
- Eusuf, M. S. R. S., Barton, J., Gorte, B., Zlatanova, S., 2020. Volume estimation of fuel load for hazard reduction burning: First results to a voxel approach. *ISPRS - International Archives of the Photogrammetry, Remote Sensing and Spatial Information Sciences*, XLIII-B3-2020, 1199-1206.
- Homainejad, N., Zlatanova, S., Pfeifer, N. 2022, A voxel-based method for the three-dimensional modelling of heathland from lidar point clouds: First results, *ISPRS Annals of the Photogrammetry, Remote Sensing and Spatial Information Sciences*, 05/17, 697-704.
- Humphreys, M. A., Rijal, H. B., Nicol, J. F., 2013. Updating the adaptive relation between climate and comfort indoors; new insights and an extended database. *Building and Environment*, 63, 40-55.
- Janoutová, R., Homolová, L., Malenovský, Z., Hanuš, J., Lauret, N., Gastellu-Etchegorry, J. P., 2019. Influence of 3D spruce tree representation on accuracy of airborne and satellite forest reflectance simulated in DART. *Forests*, 10(3).
- Meng, Y., Wang, X., Yang, J., Xu, H., Yue, F., 2021. Research on machine learning based model for predicting the impact status of laminated glass. *Wuji Cailiao Xuebao/Journal of Inorganic Materials*, 36(1), 61-68.
- Ortega-Córdova, L., 2018. *Urban Vegetation Modeling 3D Levels of Detail*. Maaster Delft University of Technology.
- Pan, Z., Yang, J., Wang, X. E., Wang, F., Azim, I., Wang, C., 2021. Image-based surface scratch detection on architectural glass panels using deep learning approach. *Construction and Building Materials*, 282.
- Rupp, R. F., Parkinson, T., Kim, J., Toftum, J., de Dear, R., 2022. The impact of occupant's thermal sensitivity on adaptive thermal comfort model. *Building and Environment*, 207.
- Sepasgozar, S., Wang, C., Shirowzhan, S., 2016: *Challenges and Opportunities for Implementation of Laser Scanners in Building Construction*.
- Shirowzhan, S., Sepasgozar, S. M. E., Zaini, I., Wang, C. 2017, An integrated GIS and Wi-Fi based Locating system for improving construction labor communications, *ISARC 2017 - Proceedings of the 34th International Symposium on Automation and Robotics in Construction*, Scopus, 1052-1059.
- Stewart, I. D., Oke, T., 2012. Local climate zones for urban temperature studies. *Bulletin of the American Meteorological Society*, 93, 1879-1900.
- Tsoka, S., Tsikaloudaki, A., Theodosiou, T., 2018. Analyzing the ENVI-met microclimate model's performance and assessing cool materials and urban vegetation applications—A review. *Sustainable Cities and Society*, 43, 55-76.
- U.S. Department of Energy, 2022. *Weather Data By Location All Regions - Southwest Pacific (WMO Region 5) - Australia*. Available at: [https://energyplus.net/weather-location/southwest\\_pacific\\_wmo\\_region\\_5/AUS/AUS\\_NSW.Sydney.947680\\_RMY](https://energyplus.net/weather-location/southwest_pacific_wmo_region_5/AUS/AUS_NSW.Sydney.947680_RMY) [Accessed 8 May 2022].
- Wang, C., Sepasgozar, S., Wang, M., Sun, J., Ning, X., 2019. Green performance evaluation system for energy-efficiency-based planning for construction site layout. *Energies*, 12, 4620.
- Wang, C., Zamri, M., 2013: *Effect of IEQ on Occupant Satisfaction and Study/Work Performance in a Green Educational Building: A Case Study*.
- Wang, M., Wang, C., Sepasgozar, S., Zlatanova, S., 2020a. A systematic review of digital technology adoption in off-site construction: Current status and future direction towards industry 4.0. *Buildings*.
- Wang, X. E., Meng, Y., Yang, J., Huang, X., Wang, F., Xu, H., 2021a. Optimal kernel extreme learning machine model for predicting the fracture state and impact response of laminated glass panels. *Thin-Walled Structures*, 162.
- Wang, Y., Cheng, Y., Zlatanova, S., Palazzo, E., 2020b. Identification of physical and visual enclosure of landscape space units with the help of point clouds. *Spatial Cognition and Computation*, 20(3), 257-279.
- Wang, Y., Zlatanova, S., Yan, J., Huang, Z., Cheng, Y., 2021b. Exploring the relationship between spatial morphology characteristics and scenic beauty preference of landscape open space unit by using point cloud data. *Environment and Planning B: Urban Analytics and City Science*, 48(7), 1822-1840.
- Xu, H., Wang, C. C., Shen, X., Zlatanova, S., 2021a. 3D tree reconstruction in support of urban microclimate simulation: A comprehensive literature review. *Buildings*, 11(9).
- Xu, Y., Shen, X., Lim, S., 2021b. CorDet: Corner-aware 3D object detection networks for automated scan-to-bim. *Journal of Computing in Civil Engineering*, 35(3).
- Xu, Y., Shen, X., Lim, S., Li, X., 2021c. Three-dimensional object detection with deep neural networks for automatic as-built reconstruction. *Journal of Construction Engineering and Management*, 147(9).
- Yang, S., Zhou, D., Wang, Y., Li, P., 2020. Comparing impact of multi-factor planning layouts in residential areas on summer thermal comfort based on orthogonal design of experiments (ODOE). *Building and Environment*, 182.